Journal of Umm Al-Qura University for Medical Sciences

Journal homepage: https://uqu.edu.sa/en/mj

Research Article

Transit time spectrum dependence upon ultrasound input wave types propagating through liquid: solid replica models, a simulation study

Saeed M. Alqahtani[*1], Ali H. Alomari[2], Marwan A. Althomali[1]
Physics Department, College of Applied Science, Umm Al-Qura University, Makkah, Saudi Arabia[1]
Physics Department, Al-Qunfudah University College, Umm Al-Qura University, Makkah, Saudi Arabia[2]

ARTICLE INFO

Received: 17/11/2022
Revised: 24/12/2022
Accepted: 04/02/2023

Keywords:
Ultrasound, Transit time spectroscopy, Ultrasound propagation, Composite media, Deconvolution

***Corresponding author:**
Saeed M. Alqahtani
E: smqahtani@uqu.edu.sa
DOI:https://doi.org/10.54940/ms45313008

ABSTRACT

BACKGROUND: Ultrasound transit time spectroscopy (UTTS) has been introduced previously to characterize the propagation of ultrasound waves through complex structures such as cancellous bone to estimate bone quality and quantity. UTTS describes the propagation of ultrasonic waves through a medium with two components of differing sound speeds (e.g., bone and marrow) as a set of parallel sonic rays. The transit time spectrum (TTS) is derived via the digital deconvolution of the input and output signals.

Aim of the study is to investigate the dependence of TTS upon the type of ultrasound input wave, including four different 1 MHz ultrasound waves (pulse, chirp, tone-burst, and continuous).

METHODS: Ten replica 3D- acrylic step-wedge models with different structure complexity were investigated. For each model and using the four types of input waves, TTS was derived and compared with calculated TTS based on the parallel sonic ray concept.

RESULTS: The results showed coefficients of determination (R^2) of 0.994, 0.999, 0.90, and 1 for pulse, chirp, tone-burst and continuous signals respectively. Furthermore, solid volume fraction (SVF) was derived via TTS (TTS-SVF) and compared with the geometrically calculated SVF data of the models, yielding coefficients of determination (R^2) of 0.941, 0.968, 0.489, and 0.981 for pulse, chirp, tone-burst and continuous waves, respectively. Therefore, the continuous wave provided a more accurate prediction of TTS and SVF, followed by chirp, then pulse waves.

CONCLUSION: This study adds to the body of research supporting the validity and reliability of UTTS, as a potentially promising technique to provide a reliable in vivo estimate of bone mineral density.

1. INTRODUCTION

Osteoporosis is a skeletal disease represented by a significant decrease in the bone mass with deterioration of the cancellous bone microarchitecture; leading to bone weakness and increasing fracture risk (Peña & Perez, 2012; Sambrook & Cooper, 2006). It is a worldwide health issue that mainly affects elderly people. After the age of 60, one in two women and one in three men will experience a fracture because of osteoporosis (Langton, 2011). As a result, developing diagnostic techniques are crucial to assess and forecast osteoporotic fracture risk factors and reduce the related mortality and disability.

Bone mineral density (BMD) is the gold standard for determining bone status and the severity of osteoporosis (Ayub et al., 2021; Johansson et al., 2009; Schuit et al., 2004; Stone et al., 2003). DXA is based on using X-rays with two different energies, usually 40 and 70 keV. The intensity of the X-rays and the attenuation coefficients of bone and soft tissue are used to calculate the value of BMD (Gefen, 2005). This is typically assessed by DXA at osteoporosis-prone skeletal locations at the spine, hip, and wrist. QCT is another X-ray-based osteoporosis assessment technique that measures volumetric bone mineral density (vBMD, in g cm^{-3}), where both the trabecular and cortical bone may be evaluated independently (Chiba et al., 2022; Yerges et al., 2010).

However, both DXA and QCT have some drawbacks such as their excessive cost, bulky equipment size and limited availability in rural and less developed areas. In addition, both modalities expose patients to ionizing radiation, but the absorbed dose from QCT is 10 times greater than that from DXA, which limits its use as a routine assessment for osteoporosis (Njeh et al., 1999). Thus, developing an effective, simple, cheap, and non-ionizing technique is important.

Quantitative ultrasound (QUS) is an alternative technique to X-ray-based methods and is widely used to study the dependence of ultrasound parameters upon bone density and structure (Fuerst et al., 1995; Trimpou et al., 2010). The fundamental principle of QUS is the measurement of two main ultrasonic parameters; Broadband Ultrasound Attenuation (BUA, dB/MHz) and Speed of Sound (SOS, m/s). Other valuable ultrasound metrics have been developed showing a potential impact on the assessment of osteoporotic fractures such as frequency-dependent Backscatter Coefficient (BSC), Apparent Integrated Backscatter (AIB), Osteoporosis Score (OS), Integrated Reflection Coefficient (IRC), Broadband Ultrasound Backscatter (BUB) and Fragility Score (F.S.)(Pisani et al., 2017). The calcaneus (heel) is the most popular anatomical site for the clinical evaluation of QUS parameters due to its high metabolic rate and high proportion of trabecular bone (Hauff et al., 2008). Several cross-sectional and prospective studies investigate QUS's discriminating ability for predicting fracture risk. According to several studies, QUS may have a similar discrimination of fracture risk as DXA. Hans et al. found that calcaneal QUS decreased with fracture risk (Hans et al., 1996). Moayyeri et al. evaluated 21 prospective studies, including 55,164 women and 13,742 men, and figured out that the ability of QUS to predict fracture risk is the same as that of DXA (Moayyeri et al., 2012). In a prospective cohort study of 62 diabetic patients with various comorbidities, QUS calcaneus bone density exhibited a high correlation with DXA hip bone density (Anna et al., 2021). Moreover, QUS parameters were found to be even better at predicting osteoporotic fracture risk than aBMD assessed by DXA (Chan et al., 2012; Gonnelli et al., 2005; Viswanathan et al., 2018). Compared to DXA and QCT, QUS is non-ionizing, cost-effective, simple to use, and has the potential capability of determining bone microarchitectures as a veritable indicator of bone strength (de Oliveira, Mario A and Moraes, Raimes and Castanha, Everton B and Prevedello, Alexandra S and Jozue Filho, V and Bussolaro, Frederico A and Cava, 2022; Krieg et al., 2008; Wang et al., 2006). However, QUS is not frequently used to determine osteoporotic individuals since the propagation of ultrasound through complicated structures such as cancellous bone is not well understood.

Several hypotheses have attempted to explain the relationship between physical ultrasonic parameters and bone density and structure, such as those proposed by Biot (Biot, 1956) and Schoenberg (Schoenberg, 1984). In 2011, Langton proposed that phase interference induced by heterogeneity in the transit times of the propagating sonic rays is the fundamental ultrasonic attenuation mechanism in cancellous bone (Langton, 2011).

This has led to the development of a novel analytical method called Ultrasound Transit Time Spectroscopy (UTTS). This method describes ultrasound propagation as an array of parallel sonic rays and the transit time of each sonic ray is determined by the relative proportion of the two constituents of differing propagation velocities; for example, bone tissue and marrow, regardless of the sample's structure. Therefore, minimum transit time (t_{min}) and maximum (t_{max}) correspond to the propagation of a sonic ray through the entire bone and marrow, respectively. In addition, UTTS describes the proportion of sonic rays ($P(t_i)$) having a particular transit time (t_i) between t_{min} and t_{max} (Langton, 2011; Langton & Wille, 2013). The received ultrasound signal is a superposition of all sonic rays, making the determination of the sample structure infeasible. The primary cause is phase interference between all sonic rays, while reflection and refraction are considered to have less influence (Alomari, Ali and Langton, 2023). Phase interference is considered as temporal and spatial. Temporal phase interference (Figure 1a) exists when the transit time difference (dt) between two or more sonic rays is less than the pulse width (W = n.T, where n is the number of pulses and T is the pulse period) of a propagated signal. Spatial phase interference (Figure 1b) occurs when the lateral dimension of the receive transducer aperture (dL) is greater than the lateral separation (ds) of the received sonic rays of differing transit times (Al-Qahtani, Saeed M and Langton, 2016).

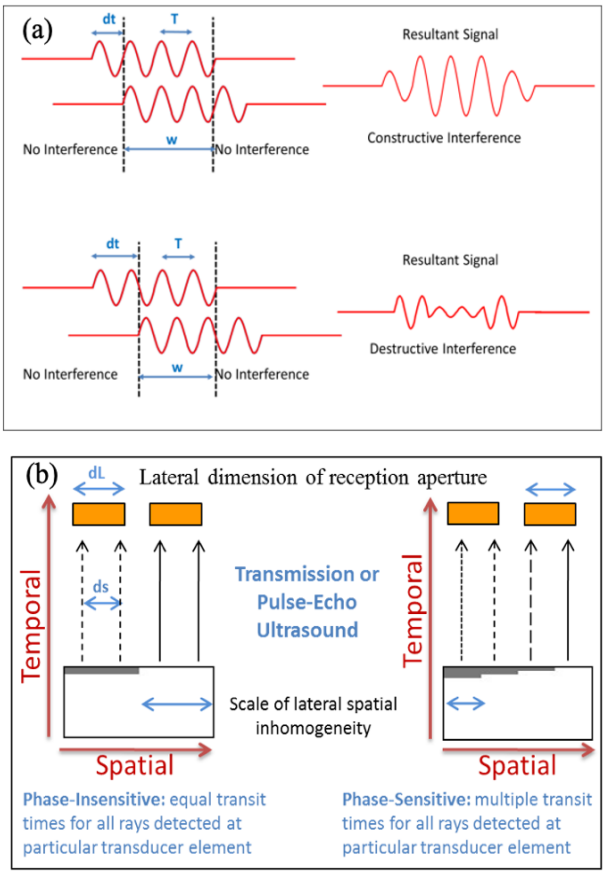

Figure 1: (a): Temporal Criterion: difference in transit-time of two (or more) sonic rays is less than the pulse length (dt < n.T). (b) Spatial Criterion: two (or more) sonic rays of differing transit-time detected within same aperture (lateral spatial inhomogeneity).

UTTS is derived by deconvolving two recorded ultrasound signals that propagate through two distinct media: the reference ultrasound signal amplitude (often through water) and the ultrasound output signal (through the sample) (Langton et al., 2014). The concept of UTTS has been validated in transmission (Langton & Wille, 2013) and pulse echo (Wille et al., 2016) modes. Validation of the TTS deconvolution technique has successfully led to estimate the volume fraction of solid: liquid (Alomari et al., 2017; Wille & Langton, 2015b) and liquid: liquid (Al-Qahtani & Langton, 2016) composites as well as improvement in image axial resolution (M. Almualimi et al., 2018; M. A. Almualimi et al., 2019) UTTS could effectively estimate the bone volume to tissue volume ratio (BV/TV) and numerous structural characteristics of cancellous bone samples (Alomari et al., 2018). Furthermore, UTTS could successfully estimate areal and volumetric BMD for 12 human cancellous bone samples (Alomari et al., 2021).

The aim of this simulation study is to investigate the dependence of UTTS upon the characteristics of ultrasound input waves using varying structures of different complexity.

2. MATERIALS AND METHODS

2.1. Ultrasound signals

Computer simulation was performed using Matlab software (Matlab 2020, MathWorks Inc., Natick, MA, USA) replicating the study conducted by Langton and Marie (Langton & Wille, 2013). However, four different 1MHz ultrasound waves (pulse, chirp, tone-burst and continuous) were generated and utilized as an input signal (i(t)) as shown in Figure 2. All input signals are sinusoidal waves. A single cycle is known as a pulse signal and multicycle waves are considered continuous, while tone-burst signal is generated from multiple pulses with offsets for each, creating a Gaussian shape. A chirp signal is a pulse signal of increasing or decreasing frequency and amplitude ranging from 0.5 to 2 MHz with a central frequency of 1 MHz.

2.2. Samples

The simulation implemented ten cylindrical acrylic step-wedge samples, with a diameter of 25 mm and a total thickness of 20 mm, made of acrylic and water (simplified bone: marrow surrogates). The structures of samples exhibit varying complexity, as shown in Figure 3. The sample complexity was attained by varying the thickness of the acrylic composite of one dimension perpendicular to the wave propagation direction, exhibiting inhomogeneous transit times. Thus, various step-wedge shape models of acrylic were designed by increasing the number of steps n, from one step (totally acrylic, Figure 3, b) to twenty steps (Figure 3, k), while minimizing the step height (l). The samples used in this study are in order as shown in Figure 3 (b-bone, c-normal, d-parallel, e-75% bone, f-75% marrow, g-W3, h-W4, i-W5, j-W10, k-W20).

Information for each signal/sample for the various parameters is summarized in Table 1.

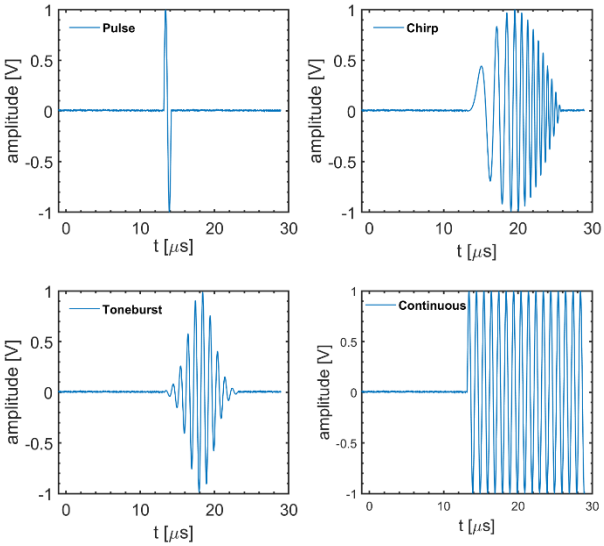

Figure 2: 1MHz pulse, chirp, tone-burst and continuous ultrasonic signals in time domain.

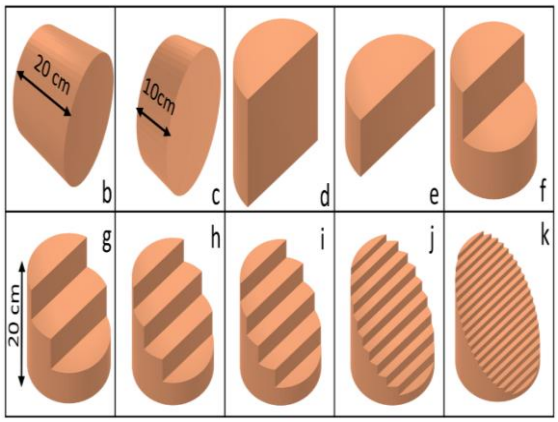

Figure 3: A sketch of the acrylic step-wedge samples, where the reference model (a), which consisted of just water, is not shown.

Table 1: Samples and input signal parameters

Samples parameters				Input signals parameters	
Sample	Number of steps (n)	Step height (*l*) (mm)	TT dela(dt) μs	Type	Pulse width (μs)
b	1	20	0	pulse	1
c	1	10	0		
d	2	20	5.71	chirp	12.7
e	2	10	2.87		
f	2	10	2.81	tone-burst	9.92
g	3	6.66	1.92		
h	4	5	1.43	continuous	15.93
i	5	3.33	1.13		
j	10	2	0.57		
k	20	1	0.28		

2.3. Derivation of ultrasound output signal

The simulated output ultrasonic signal was simulated using Matlab software (MathWorks Inc., Natick, MA, USA) through applying several propagation factors, including signal transit time, relative area and relative absorption. Firstly, the transit time (t_i) of each step-wedge was determined as the amount of solid and liquid each sonic ray propagates through and can be calculated as:

$$t_i = [(d_a/v_a)] + [(d_w/v_w)] \quad (1)$$

Where d_a and d_w are the thicknesses of acrylic and water respectively. v_a and v_w correspond to ultrasound velocities through acrylic and water, which have been experimentally measured to be (2614.5 ± 9.1 ms^{-1}) and (1485.5 ± 2.1 ms^{-1}), respectively (Al-Qahtani et al., 2018).

Secondly, we consider uniform planer wave propagation over the entire cross-section of the samples, and hence, the proportion of sonic rays corresponding to a specific step-wedge is mismatched and governed by the relative area as described previously (Al-Qahtani et al., 2018) using the following equations;

$$A = \frac{R^2\,(\theta - \sin\theta)}{2} \quad (2)$$

where; $\theta = 2.arcos\left(\frac{R-h}{R}\right)$

Where R represents the disc's radius, h the segment's height, and θ the angle subtended by the segment.

Thirdly, a relative attenuation factor was introduced for each step depending on the thickness of its solid component. This was determined using the conventional equation [$A_x = A_0\, e^{-\mu x}$], where A_0 and A_x are the signal amplitudes at distances of zero and x, respectively, where x is the thickness of the disc and μ is the attenuation coefficient of acrylic material, which equals 25.3 Np/m as reported in (Langton & Wille, 2013).

Thus, by applying these three correcting factors, the simulated output signals (o(t)) for the nth (where n = 1 - 20) step-wedge sample may be written as follows:

$$simulated\ o(t) = i(t) * t_n * A_n * exp^{-\mu x_n} \quad (3)$$

2.4. Derivation of UTTS Through Deconvolution

Active-set deconvolution algorithm developed by Landi and Zama in 2006 (Landi & Zama, 2006) was implemented to derive the transit time spectrum (TTS) by deconvoluting the simulated ultrasound input and output signals. This technique has been previously described and approved by Langton et al. (Al-Qahtani et al., 2018; Langton et al., 2014; Wille & Langton, 2015b), as follows;

$$TTS = F^{-1}\left[\frac{O(\omega)}{I(\omega)}\right] \quad (4)$$

where O(ω), and I(ω) are the Fourier transforms of the output and input signals, respectively.

2.5. Solid Volume Fraction Determination

The solid volume fraction (SVF) is the portion of solid volume (SV) to total volume (TV) of test samples (SVF = SV/TV). This can be calculated, as a reference, by physical measurement with a digital clipper, based on the sample geometrical parameters of sample diameter, step width and step height.

For computer simulation, the solid proportion ($SP(t_i)$) of sonic rays at a specific transit time (t_i) can be determined as;

$$SP(t_i) = 1 - \left[\frac{t_i - t_{min}}{t_{max} - t_{min}}\right] \quad (5)$$

Where t_{min} and t_{max} are the transit times through the entirety of acrylic and water, respectively, from which the SVF can be determined by the integration of the product of each solid proportion with its corresponding sonic ray proportion $P(t_i)$ of transit time (t_i) as follows;

$$SVF = \sum_{t_{min}}^{t_{max}} SP(t_i) \cdot P(t_i) \quad (6)$$

However, the proportion of a sonic ray depends on the amplitude of the received simulated output signal which is subject to material absorption. Therefore, $P(t_i)$ is underestimated, and hence, an absorption correction factor was applied as follows, based on the published work by (Alomari et al., 2021).

$$AC\ (t_i) = 1/e^{-(\mu_a \cdot [(t_i - x_s/v_W)/(1/v_b - 1/v_W)])} \quad (7)$$

Where μ_a is the attenuation/ absorption coefficient of the acrylic material assumed to be 25.3 Np m^{-1} at 1 MHz (based upon Perspex attenuation of 57 Np m^{-1} reported at 2.25 MHz (Laby & Kaye, 2005), being analogous to acrylic, assuming a linear dependence with frequency) (Bauer et al., 2008; Chaffa, S and Peyrin, F and Nuzzo, S and Porcher, R and Berger, G and Laugier, 2002). Moreover, x_s [$x_s = x_a + x_w$] is a sample thickness (where x_a, x_w are acrylic and water thicknesses) for a given transit time (t_i), from which the corrected sonic ray proportion can be determined as:

$$P_{corr}(t_i) = P(t_i) \cdot AC(t_i) \quad (8)$$

Thus, the corrected SVF can be estimated as:

$$SVF = \sum_{t_{min}}^{t_{max}} SP(t_i) \cdot P_{corr}(t_i) \quad (9)$$

The simulated derived SVF was then compared to the calculated SVF for further analysis.

2.6. Data Analysis

A linear regression model using MATLAB software was used to calculate the coefficient of determination (R^2) between; a) the calculated and simulated TTS and b) the calculated and simulated SVF values.

3. RESULTS

The aim of this paper was to investigate whether the transit time spectrum of propagated ultrasound waves through complex media, exhibiting different complexities and levels of phase interference, depends on the input ultrasound wave characteristics.

Four different 1MHz input signals (pulse, chirp, tone-burst and continuous) were simulated through 10 step-wedge acrylic samples to derive the output signals. Through deconvolution of the "input" and simulated "output" ultrasound signals, a transit time spectrum was derived. Figure 4 shows qualitative comparisons between calculated (dashed red) and derived (solid black) TTS of the four different input signals for all samples.

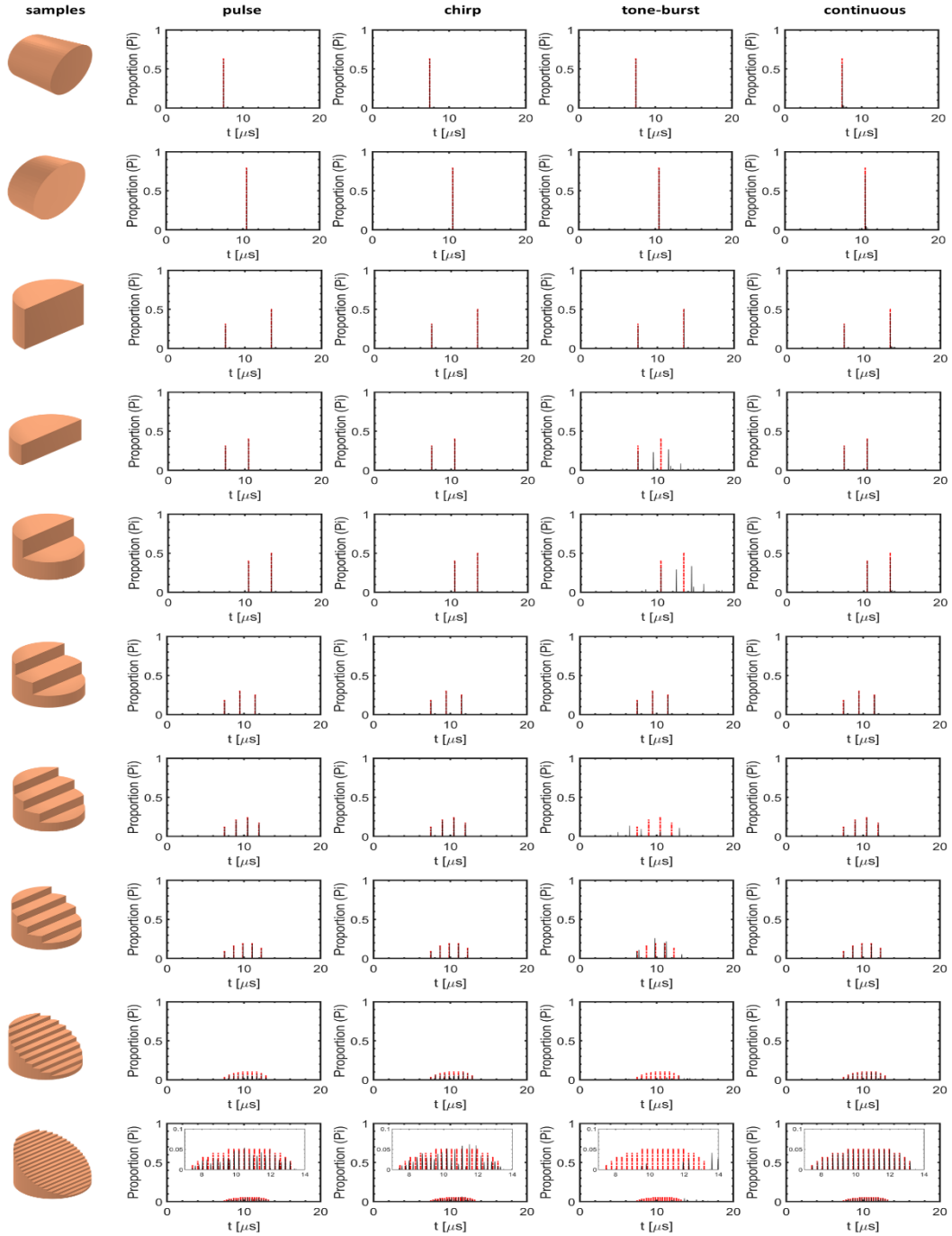

Figure 4: Qualitative comparisons between calculated (dashed red) and derived (solid black) TTS of the four different input signals for all samples.

Plots in Figure 4 clearly indicate high similarity between calculated and derived TTS formats for pulse, chirp, and continuous signals. However, tone-burst plots possess less similarity in both (t_i) and P(t_i) components, particularly in more complex structures, as evidenced by h, I, J and k models.

These observations were confirmed by quantitative comparisons using correlation analysis tests between calculated and derived transit times (t_i) as presented in Figure 5. The coefficients of determination (R^2) were 0.998, 0.991, 0.90 and 1 for pulse, chirp, tone-burst and continuous signals, respectively. The highest correlations were again for pulse, chirp, continuous signals. Interestingly, although a chirp signal is a varying-frequency signal, it provided a high R^2 value of 0.991. This supports a previous study concluding that TTS is frequency-independent (Wille & Langton, 2015a). Regarding tone-burst signals, although the correlation is strong (R^2 = 0.90), it is the lowest among the four signals, and this needs further investigation.

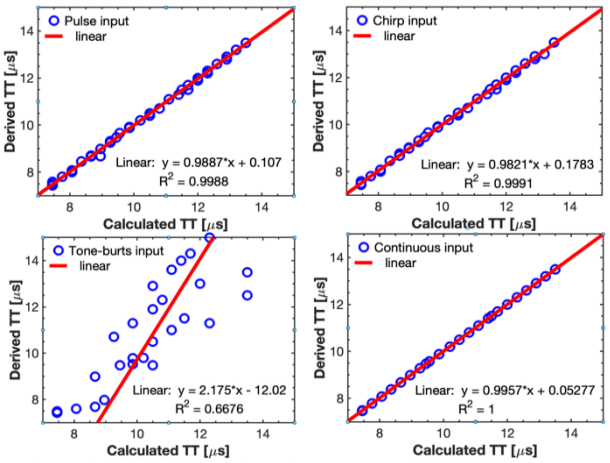

Figure 5: Correlation analyses between calculated and derived TTS spectra.

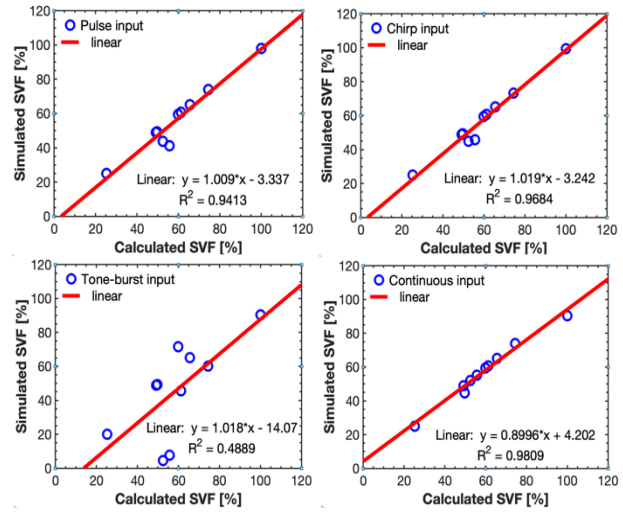

Figure 6: Correlation analyses between calculated and derived SFV.

One method to examine the accuracy of deriving the transit time spectrum of propagated ultrasound through binary composite structures is through determining SVF, which has been studied previously (Alomari et al., 2018, 2021) In this study, the derived TTS-SVF was estimated using Equation 9 for each sample using the four types of input signals. Figure 6 shows the correlation analyses between the geometrically calculated SVF and derived TTS-SVF for all input signals, yielding a coefficient of determination (R^2) of 0.941, 0.968, 0.489 and 0.981 for pulse, chirp, tone-burst and continuous signals respectively. The highest correlation was for a continuous signal (R^2 = 0.981), followed by a chirp signal (R^2 = 0.968). This might be attributed to the low signal-to-noise ratio in these signals, allowing for deriving accurate (t_i) and P(t_i) values. The tone-burst signal provided again the lowest correlation (R^2 = 0.489), which requires more investigation.

Although promising results have been obtained, this study is limited to the use of replica samples, which do not represent natural tissues. Furthermore, only 1 MHz simulated input signals have been investigated, and thus experimental signals with different frequencies might further confirm the findings of this study. Despite the limitations, it is anticipated that UTTS has shown a reliable ability to estimate the SVF of 10 step-wedge samples using input signals with varied characteristics.

4. CONCLUSION AND RECOMMENDATION

This study aimed to investigate the effect of ultrasonic input/output signal types upon UTTS. The achieved results showed that a continuous signal provided more accurate prediction of TTS and SVF, followed by chirp, then pulse signals. However, the lower results were obtained by tone-burst signals, and thus further investigations are required. It is therefore assumed that UTTS is a potentially accurate and independent technique for bone assessment.

AUTHOR CONTRIBUTION

All authors were involved in conceptualization, study design, searching of literature, and preparation of the manuscript. All authors have read and approved the final article.

SOURCE OF FUNDING

This research did not receive any specific grant from funding agencies in the public, commercial, or non-profit sectors.

CONFLICT OF INTEREST

The authors have no conflicts of interest to declare.

ACKNOWLEDGEMENTS

The author would like to thank Prof. Dr. Christian Langton (Griffith University – Australia) for critical revision of the manuscript.

REFERENCES

Almualimi, M. A., Al-Qahtani, S., Wille, M. L., & Langton, C. M. (2019). Improvement of B-scan spatial resolution by pulse-echo ultrasound transit time spectroscopy. *Applied Acoustics*, *145*, 193–204. https://doi.org/10.1016/j.apacoust.2018.10.012

Almualimi, M., Wille, M.-L., & Langton, C. M. (2018). Potential for ultrasound transit time spectroscopy to improve axial resolution. *Applied Acoustics*, *133*, 91–96.

Alomari, A. H., Al-Qahtani, S. M., & Langton, C. M. (2021). In-vitro comparison of volumetric and areal bone mineral density measurements between ultrasound transit time spectroscopy and microcomputed tomography. *Applied Acoustics*, *179*, 108072.

Alomari, A. H., Wille, M.-L., & Langton, C. M. (2017). Soft-tissue thickness compensation for ultrasound transit time spectroscopy estimated bone volume fraction—an experimental replication study. *Biomedical Physics & Engineering Express*, *3*(4), 45013.

Alomari, A. H., Wille, M.-L., & Langton, C. M. (2018). Bone volume fraction and structural parameters for estimation of mechanical stiffness and failure load of human cancellous bone samples; in-vitro comparison of ultrasound transit time spectroscopy and X-ray μCT. *Bone*, *107*, 145–153.

Alomari, A., and Langton, C. (2023). Comparison of deconvoluted-convoluted reconstituted ultrasound signals with their experimental original in a porous composite, cancellous bone. *Journal of Radiation Research and Applied Sciences*, *16*(1), 100519.

Al-Qahtani, S. M., & Langton, C. M. (2016). Estimation of liquid volume fraction using ultrasound transit time spectroscopy. *Measurement Science and Technology*, *27*(12). https://doi.org/10.1088/0957-0233/27/12/125003

Al-Qahtani, S. M., Wille, M.-L., & Langton, C. M. (2018). Transducer impulse response correction for a deconvolution derived ultrasound transit time spectrum. *Physics in Medicine & Biology*, *63*(17), 175009.

Al-Qahtani, Saeed M., and Langton, C. M. (2016). Ultrasound temporal-spatial phase-interference in complex composite media; A comparison of experimental measurement and simulation prediction. *Ultrasonics*, *71*, 115–126. https://doi.org/10.1016/j.ultras.2016.06.001

Anna, U., Maria, S., Practice, B. K.-D. R. and C., & 2021, U. (2021). Comparison of quantitative ultrasound of calcaneus and dual energy X-ray absorptiometry in measuring bone density and predicting fractures in patients with. *Diabetes Research and Clinical Practice*, *180*, 109064.

Ayub, N., Faraj, M., Ghatan, S., Reijers, J. A. A., Napoli, N., Oei, L., & Valderrabano, V. (2021). The treatment gap in osteoporosis. *Journal of Clinical Medicine*, *10*(13), 3002. https://doi.org/10.3390/jcm10133002

Bauer, A. Q., Marutyan, K. R., Holland, M. R., & Miller, J. G. (2008). Negative dispersion in bone: the role of interference in measurements of the apparent phase velocity of two temporally overlapping signals. *Journal of the Acoustical Society of America*, *123*(4), 2407–2414.

Biot, M. A. (1956). Theory of propagation of elastic waves in a fluid-saturated porous solid. II. higher frequency range. *Journal of the Acoustical Society of America*, *28*(2), 179–191.

Chaffa, S and Peyrin, F and Nuzzo, S and Porcher, R and Berger, G and Laugier, P. (2002). Ultrasonic characterization of human cancellous bone using transmission and backscatter measurements: relationships to density and microstructure. *Bone*, *30*(1), 229–237. https://doi.org/10.1016/s8756-3282(01)00650-0

Chan, M. Y., Nguyen, N. D., Center, J. R., Eisman, J. A., & Nguyen, T. V. (2012). Absolute fracture-risk prediction by a combination of calcaneal quantitative ultrasound and bone mineral density. *Calcified Tissue International*, *90*(2), 128–136. https://doi.org/10.1007/s00223-011-9556-3

Chiba, K., Osaki, M., & Ito, M. (2022). Assessment of Osteoporosis by QCT, HR-pQCT, and MRI. In *Osteoporotic Fracture and Systemic Skeletal Disorders* (pp. 177–185). Springer Singapore. https://doi.org/10.1007/978-981-16-5613-2_11

de Oliveira, Ma A and Moraes, Raimes and Castanha, Everton B and Prevedello, Alexandra S and Jozue Filho, V and Bussolaro, Frederico A and Cava, D. G. (2022). Osteoporosis Screening: Applied Methods and Technological Trends. *Medical Engineering & Physics*, 103887.

Fuerst, T., Glüer, C. C., & Genant, H. K. (1995). Quantitative ultrasound. *European Journal of Radiology*, *20*(3), 188–192.

Gefen, A. (2005). Langton CM, Njeh CF, (eds): The Physical Measurement of Bone. *BioMedical Engineering OnLine 2005 4:1*, *4*(1), 1–3. https://doi.org/10.1186/1475-925X-4-37

Gonnelli, S., Cepollaro, C., Gennari, L., Montagnani, A., Caffarelli, C., Merlotti, D., Rossi, S., Cadirni, A., & Nuti, R. (2005). Quantitative ultrasound and dual-energy X-ray absorptiometry in the prediction of fragility fracture in men. *Osteoporosis International*, *16*(8), 963–968. https://doi.org/10.1007/S00198-004-1771-6

Hans, D., Dargent-Molina, P., Schott, A. M., Sebert, J. L., Cormier, C., Kotzki, P. O., Delmas, P. D., Pouilles, J. M., Breart, G., & Meunier, P. J. (1996). Ultrasonographic heel measurements to predict hip fracture in elderly women: the EPIDOS prospective study. *The Lancet*, *348*(9026), 511–514.

Hauff, P., Reinhardt, M., & Foster, S. (2008). Ultrasound Basics. In W. Semmler & M. Schwaiger (Eds.), *Molecular Imaging I: Vol. 185/1* (pp. 91–107). Springer Berlin Heidelberg. https://doi.org/10.1007/978-3-540-72718-7_5

Johansson, H., Kanis, J. A., Odén, A., Johnell, O., & McCloskey, E. (2009). BMD, clinical risk factors and their combination for hip fracture prevention. *Osteoporosis International*, *20*(10), 1675–1682.

Krieg, M.-A., Barkmann, R., Gonnelli, S., Stewart, A., Bauer, D. C., Barquero, L. D. R., Kaufman, J. J., Lorenc, R., Miller, P. D., & Olszynski, W. P. (2008). Quantitative ultrasound in the management of osteoporosis: the 2007 ISCD Official Positions. *Journal of Clinical Densitometry*, *11*(1), 163–187.

Laby, T. H., & Kaye, G. W. C. (2005). The speed and attenuation of sound. In *Tables of Physical & Chemical Constants*. Kaye Laby Online.

Landi, G., & Zama, F. (2006). The active-set method for nonnegative regularization of linear ill-posed problems. *Applied Mathematics and Computation*, *175*(1), 715–729. https://doi.org/10.1016/j.amc.2005.07.037

Langton, C. M. (2011). The 25th anniversary of BUA for the assessment of osteoporosis: time for a new paradigm? *Engineering in Medicine*, *225*(2), 113–125. https://doi.org/10.1243/09544119jeim777

Langton, C. M., & Wille, M. L. (2013). Experimental and computer simulation validation of ultrasound phase interference created by lateral inhomogeneity of transit time in replica bone: marrow composite models. *Proc Inst Mech Eng H*, *227*(8), 890–895. https://doi.org/10.1177/0954411913486079

Langton, C. M., Wille, M. L., & Flegg, M. B. (2014). A deconvolution method for deriving the transit time spectrum for ultrasound propagation through cancellous bone replica models. *Proc Inst Mech Eng H*, *228*(4), 321–329.

Moayyeri, A., Adams, J. E., Adler, R. A., Krieg, M. A., Hans, D., Compston, J., & Lewiecki, E. M. (2012). Quantitative ultrasound of the heel and fracture risk assessment: an updated meta-analysis. *Osteoporosis International*, *23*(1), 143–153. https://doi.org/10.1007/s00198-011-1817-5

Njeh, C. F., Fuerst, T., Hans, D., Blake, G. M., & Genant, H. K. (1999). Radiation exposure in bone mineral density assessment. *Applied Radiation and Isotopes*, *50*(1), 215–236.

Peña, A. R., & Perez, V. O. (2012). *Osteoporosis: Risk Factors, Symptoms & Management*. Nova Science.

Pisani, P., Greco, A., Conversano, F., Renna, M. D., Casciaro, E., Quarta, L., Costanza, D., Muratore, M., & Casciaro, S. (2017). A quantitative ultrasound approach to estimate bone fragility: A first comparison with dual X-ray absorptiometry. *Measurement*, *101*, 243–249. https://doi.org/10.1016/J.MEASUREMENT.2016.07.033

Sambrook, P., & Cooper, C. (2006). Osteoporosis. *LANCET*, *367*(9527), 2010–2018.

Schoenberg, M. (1984). Wave propagation in alternating solid and fluid layers. *Wave Motion*, *6*(3), 303–320. https://doi.org/10.1016/0165-2125(84)90033-7

Schuit, S. C. E., Van der Klift, M., Weel, A., De Laet, C., Burger, H., Seeman, E., Hofman, A., Uitterlinden, A. G., Van Leeuwen, J., & Pols, H. A. P. (2004). Fracture incidence and association with bone mineral density in elderly men and women: the Rotterdam Study. *Bone*, *34*(1), 195–202.

Stone, K. L., Seeley, D. G., Lui, L., Cauley, J. A., Ensrud, K., Browner, W. S., Nevitt, M. C., & Cummings, S. R. (2003). BMD at multiple sites and risk of fracture of multiple types: long-term results from the Study of Osteoporotic Fractures. *Journal of Bone and Mineral Research*, *18*(11), 1947–1954.

Trimpou, P., Bosaeus, I., Bengtsson, B.-Å., & Landin-Wilhelmsen, K. (2010). High correlation between quantitative ultrasound and DXA during 7 years of follow-up. *European Journal of Radiology*, *73*(2), 360–364.

Viswanathan, M., Reddy, S., Berkman, N., Cullen, K., Middleton, J. C., Nicholson, W. K., & Kahwati, L. C. (2018). Screening to prevent osteoporotic fractures: updated evidence report and systematic review for the US Preventive Services Task Force. *Jama*, *319*(24), 2532–2551. https://doi.org/10.1001/jama.2018.6537

Wang, C., Nguyen, N., & Nguyen, T. (2006). *Quantitative ultrasound measurements and fracture risk: a review*. Clinical Publishing, An Imprint of Atlas Medical Publishing Ltd.

Wille, M.-L., Almualimi, M. A., & Langton, C. M. (2016). Pulse-echo ultrasound transit time spectroscopy: A comparison of experimental measurement and simulation prediction. *Proc Inst Mech Eng H*, *230*(1), 20–29. https://doi.org/10.1177/0954411915615911

Wille, M.-L., & Langton, C. M. (2015a). Frequency independence of ultrasound transit time spectroscopy. *5th International Conference on Biomedical Engineering in Vietnam*, 39–42.

Wille, M.-L., & Langton, C. M. (2015b). Solid volume fraction estimation of bone: marrow replica models using ultrasound transit time spectroscopy. *Ultrasonics*.

Yerges, L. M., Klei, L., Cauley, J. A., Roeder, K., Kammerer, C. M., Ensrud, K. E., Nestlerode, C. S., Lewis, C., Lang, T. F., Barrett-Connor, E., Moffett, S. P., Hoffman, A. R., Ferrell, R. E., Orwoll, E. S., & Zmuda, J. M. (2010). Candidate gene analysis of femoral neck trabecular and cortical volumetric bone mineral density in older men. *Journal of Bone and Mineral Research*, *25*(2). https://doi.org/10.1359/jbmr.090729